THE JOURNAL OF PHYSICAL CHEMISTRY B

ARTICLE

pubs.acs.org/JPCB

# Salt Effects on Condensed Protamine−DNA Assemblies: Anion Binding and Weakening of Attraction

Jason E. DeRouchey*,† and Donald C. Rau*,‡

†Department of Chemistry, University of Kentucky, Lexington, Kentucky 40506-0055, United States

‡Program in Physical Biology, National Institutes of Child Health and Human Development, National Institutes of Health, Bethesda, Maryland 20892, United States

**ABSTRACT:** Using osmotic stress coupled with X-ray scattering, we have directly examined the salt sensitivity of the intermolecular forces between helices in condensed protamine−DNA arrays. Thermodynamic forces are measured from the dependence of DNA helical interaxial spacings on external salt concentration or the osmotic pressure applied by neutral polymer solutions in equilibrium with the condensed phase. Force curves of salmon protamine−DNA condensates are highly dependent on salt species and concentration, indicating salt binding to protamine−DNA complexes. This dependence of the forces on salt species follows the Hofmeister series for anions. Chaotropic anions bind more tightly to protamine−DNA arrays than kosmotropic anions, thus more greatly disrupting the attractive thermodynamic forces. Variations with cation type are small compared with those observed for anions. Further, osmotic stress is used to estimate the number of ions bound in the condensed phase through a Gibbs−Duhem relationship. We estimate that at equilibrium, ∼1 $Br^-$ is bound per protamine molecule at 200 mM NaBr concentration. Remarkably, this one bound anion results in a change of ∼12% in the surface-to-surface distance between DNA helices. Potential biological implications of this attractive force salt sensitivity are discussed.

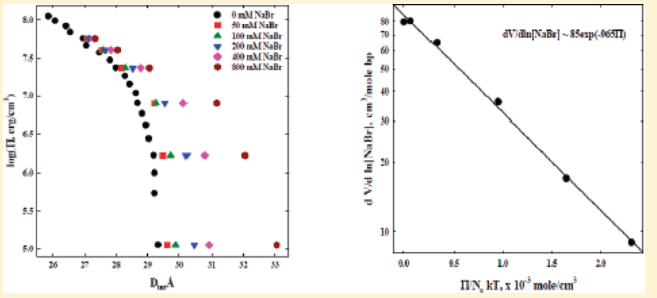


## INTRODUCTION

The packaging of highly charged DNA into tight spaces within cells is a common theme in biology. Of the eukaryotic cells, DNA is most tightly packaged in vertebrate sperm. Mouse sperm nuclei are about an order of magnitude smaller than typical somatic cell nuclei.[1−3] The DNA packaging density (v/v) in a condensed 30 nm heterochromatin fiber is approximately 25%.[4] The spacing between hexagonally packed DNA helices in stallion sperm nuclei is about 29 Å,[5] corresponding to a DNA packing density of about 45%. Attractive interactions between DNA helices mediated by bound protamine are responsible for achieving this high density. Protamines are small, arginine-rich peptides used to package DNA in vertebrate sperm.[2,6] Salmon protamine is 32 amino acids long with 21 arginines.

The attractive force between protamine−DNA helices closely resembles the forces mediated by much smaller multivalent ions, as $Mn^{2+}$, $Co(NH_3)_6^{3+}$, spermidine$^{3+}$, spermine$^{4+}$, and oligoarginines ranging from $Arg_2^{2+}$ to $Arg_6^{6+}$.[7−9] The common force characteristics indicate a common physical origin for the attraction. It seems that the protein nature of protamines is not important for DNA assembly. The equilibrium spacing between helices in condensed DNA arrays is determined by the balance of attractive and repulsive forces and typically varies from ∼7 to 15 Å of water between helices, depending on the nature of the multivalent counterion. The effect of salt on the attractive and repulsive forces in condensed arrays, however, has not been systematically investigated. The balance of forces can be varied by adding univalent salt that can screen DNA−DNA interactions and compete with the highly charged counterions for DNA binding. The DNA-bound multivalent cations can also potentially bind anions of the salt, changing the interactions between helices.

A common experiment to characterize DNA condensation is to map the phase space of precipitated and soluble DNA as a function of univalent and condensing ion concentrations.[10−16] Boundary lines are interpreted as due to a difference in the binding of univalent salt and multivalent condensing ions between the soluble and condensed DNA phases. The attractive energy gained by binding multivalent ions increases the association binding constant of these ions to DNA in the condensed phase relative to soluble DNA. At the phase transition, the interhelical attractive energy gained is balanced by the energy lost in binding the extra condensing ions necessary for condensation.[7,15] Most treatments assume the condensed phase remains constant and that the multivalent condensing ion is fully dissociated. These highly charged condensing ions, however, can also bind anions, thus greatly complicating any simple polyelectrolyte interpretation of the phase diagram. Not only can these anion-associated, multiply charged condensing ions compete with the parent ion and $Na^+$ for DNA

**Received:** April 25, 2011
**Revised:** September 2, 2011
**Published:** September 06, 2011

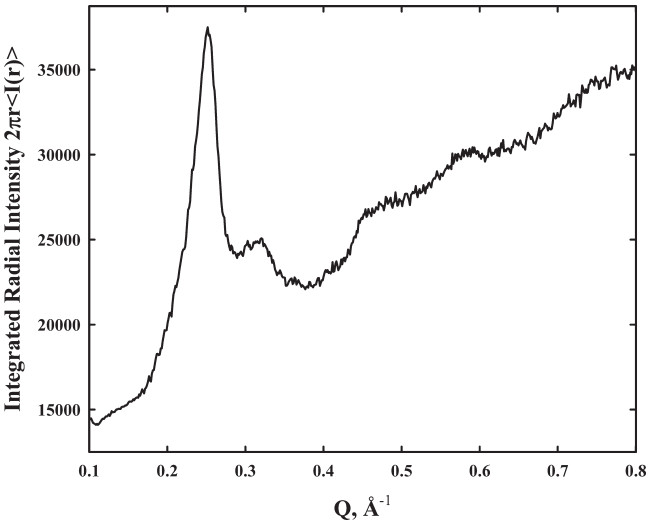


**Figure 1.** A scattering profile of a condensed protamine−DNA assembly. The radially integrated intensity, $2\pi r\langle I(r)\rangle$, is calculated from signal intensity averaged from a radius $r - 0.05$ to r + 0.05 mm and is shown as a function of Q. The intense peak at $Q = 0.24$ Å$^{-1}$ is the interaxial Bragg reflection. The position of the peak is determined by a quadratic fit to the upper third of the scattering peak after subtracting a linear baseline. The shoulder peak at slightly higher Q is the 110 reflection. Its amplitude suggests that protamine is binding in the DNA grooves. The broader peaks at even higher Q are due to higher-order reflections. The condensed protamine−DNA assembly was equilibrated against an aqueous solution of 100 $\mu$M salmon protamine in 10 mM Tris, pH 7.5.

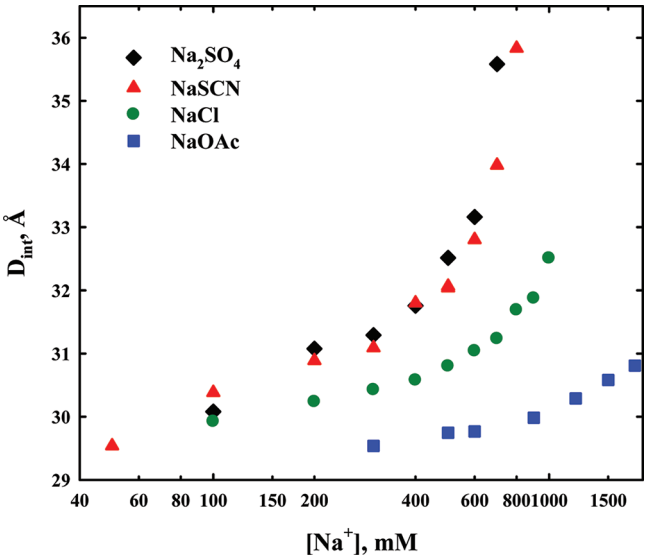


**Figure 2.** The dependence of the equilibrium spacing between protamine−DNA helices on salt concentration for $Na_2SO_4$, NaSCN, NaCl, and NaOAc. Both $Na_2SO_4$ and NaSCN cause significant swelling of protamine−DNA assemblies, even at moderate concentrations. In contrast, the interaxial spacing reaches only 30 Å at ∼1 M NaOAc, about a 10-fold higher concentration than for NaSCN. For all four salts, the DNA condensate dissolves at the next higher concentration in the series. The equilibrating solutions also contained 100 $\mu$M salmon protamine and 10 mM Tris (pH7.5).

binding in the soluble phase, but they can also lower the attractive energy gained in the condensed phase. The equilibrium spacing between helices is highly dependent on the salt concentration for DNA arrays condensed with trivalent spermidine and tetravalent spermine.[17,18] With only one type of salt, however, a general cation screening/competition mechanism cannot be distinguished from specific anion binding for explaining the weakened attraction. Anion-specific effects have been observed in DNA condensation reactions with spermidine and spermine.[18,19] The resolubilization of spermidine- and spermine-condensed DNA is likely caused by anion binding of these biogenic polyamines at high salt concentrations.[15,18]

The NaCl concentration dependence of protamine precipitation of DNA has been mapped by assaying the concentration of DNA in the soluble phase.[13] Here, we examine the effect of salt on the condensed protamine−DNA phase. The equilibrium spacing between helices in the condensed array can be determined by X-ray scattering. The forces between DNA helices with bound protamine can be measured using the osmotic stress approach. The method for direct between measurement by osmotic stress has been described previously.[20] In brief, condensed DNA arrays are equilibrated against a bathing polymer solution, typically polyethylene glycol (PEG), of known osmotic pressure. PEG is excluded from the condensed DNA phase applying a direct force on the ordered array. Water, salt, and protamine can freely exchange between the PEG and condensed DNA phases. At equilibrium, the osmotic pressure in both phases is identical. Using small-angle X-ray scattering, the interhelical spacing, $D_{int}$, is measured as a function of the applied osmotic pressure to obtain pressure-vs-distance curves. By examining protamine−DNA force curves as dependent on salt species and concentration, we can observe changes in the nature of the compacted phase due to salt.

We find that specific salt effects are surprisingly large. Anions such as $Cl^-$ bind to protamine−DNA arrays at concentrations of 0.1 M and higher and significantly weaken the attraction between helices. Chaotropic anions such as $I^-$ and $SCN^-$ bind more tightly to protamine−DNA arrays than kosmotropic anions such as acetate ($OAc^-$) and $F^-$. This binding of anions by protamine and consequent weakening of attractive forces between helices means that the salt and protamine concentration dependence of the phase diagram cannot be simply interpreted. The protamine species bound to DNA and the energetics of the condensed DNA phase change with salt concentration. Osmotic stress experiments, however, do allow us to estimate the number of bound ions in the condensed phase through a Gibbs−Duhem relationship. We find that the effect of a single bound $Br^-$ ion per protamine is remarkable, causing more than a 10% change in the equilibrium spacing between helices. The sensitivity of protamine−DNA attractive forces to anion binding has biological significance. Initially, phosphorylated protamine binds to DNA before a dephosphorylation step in spermatogenesis.[21−23] The weakened attraction of phosphorylated protamine−DNA helices may prevent tight packaging of DNA and ensure phosphatase access.

## RESULTS

At low salt concentrations and without applied PEG osmotic pressure, the spacing between helices in reconstituted salmon protamine−DNA arrays is 29.4 ± 0.1 Å. A typical X-ray scattering profile is shown in Figure 1 in standard Q-space. In terms of the total scattering angle, $2\theta$, and the X-ray wavelength, $\lambda$, Q and the Bragg spacing, $D_{Bragg}$, are defined as

$$Q = \frac{4\pi}{\lambda}\sin\theta \qquad \text{and} \qquad D_{Bragg} = \frac{2\pi}{Q} \tag{1}$$


dx.doi.org/10.1021/jp203834z |J. Phys. Chem. B 2011, 115, 11888–11894

**Table 1. Interhelical Spacings without Applied PEG Osmotic Pressure for 10 mM TrisCl, pH 7.5, and Several Different Salts at 0.5 M and in 10 mM TrisCl and 100 $\mu$M Salmon Protamine**

| salt | $D_{int}$, Å | salt | $D_{int}$, Å |
|---|---|---|---|
| 10 mM TrisCl | 29.3 | LiCl | 31.3 |
| TMAF | 29.35 | NaCl | 31.3 |
| NaF | 29.55 | $NH_4Cl$ | 31.4 |
| KF | 29.7 | LiBr | 31.6 |
| NaAc | 29.75 | NaI | 32.0 |
| CsCl | 30.45 | NaBr | 32.0 |
| KCl | 30.9 | NaSCN | 32.1 |
| TMABr | 31.2 | $Na_2SO_4$ | 32.5 |

The sharp peak at $Q \sim 0.25$ Å$^{-1}$ is the helix−helix Bragg reflection. The DNA is packed in a hexagonal array and the interaxial spacing is $D_{int} = (2/\sqrt{3})\, D_{Bragg}$. The smaller peak at slightly larger $Q$ is the 110 reflection. The amplitude of this peak is much larger than is observed for simple salts, spermidine, and spermine and suggests that protamine is binding in the grooves of DNA.[24]

Figure 2 shows the change in interhelical spacing as the salt concentration is increased for NaOAc, NaCl, NaSCN, and $Na_2SO_4$. In all these curves, the protamine concentration in the bathing solution is maintained at 100 $\mu$M with 10 mM Tris, pH 7.5. Swelling of the array is very much anion-dependent. Significant swelling occurs at even moderate concentrations of NaSCN and $Na_2SO_4$. The pellet dissolves between 0.8 and 0.9 M NaSCN. Little change in spacing is observed with NaOAc until the pellet dissolves at ~2 M. NaCl shows intermediate behavior. The sensitivity to anion species precludes salt screening or $Na^+$ ion competition with protamine binding as the principal underlying cause of the decrease in attraction. The 110 reflection gradually disappears at the higher salt concentrations, suggesting that protamine groove binding is disrupted before the pellet dissolves. The 35−36 Å interaxial reflections seen just before dissolution in NaSCN and $Na_2SO_4$ are significantly broader than for smaller spacings and may indicate a columnar to cholesteric transition.[17,25,26]

Table 1 gives spacings between helices for several salts at 500 mM concentration. There is some variation with counterion species, but the anion effect is much stronger and follows the Hofmeister series for the univalent anions. For the $Na^+$ salts, the ordering of anions is $SCN^- > I^- \sim Br^- > Cl^- > OAc^- \sim F^-$. The chaotropic anions have the greatest effect on spacing, and the kosmotropes $OAc^-$ and $F^-$ only weakly affect protamine−DNA packing. The swelling of the protamine−DNA assembly is likely due to binding of chaotropic anions, in particular, to the condensed phase.

Figure 3 shows osmotic stress force curves for protamine−DNA arrays at different NaCl concentrations. The large dependence of spacing on salt concentration seen at low PEG osmotic pressures virtually disappears at high pressures as the curves converge. As helices are pushed closer at higher osmotic pressures, $\Pi\Delta V$ work is done on the array. Since anion binding lowers the attractive energy resulting in swelling, more work will be done on the protamine−DNA array with bound $Cl^-$ than on the protamine−DNA array at constant spacing. This extra work done on the protamineCl−DNA array decreases the anion association binding constant.

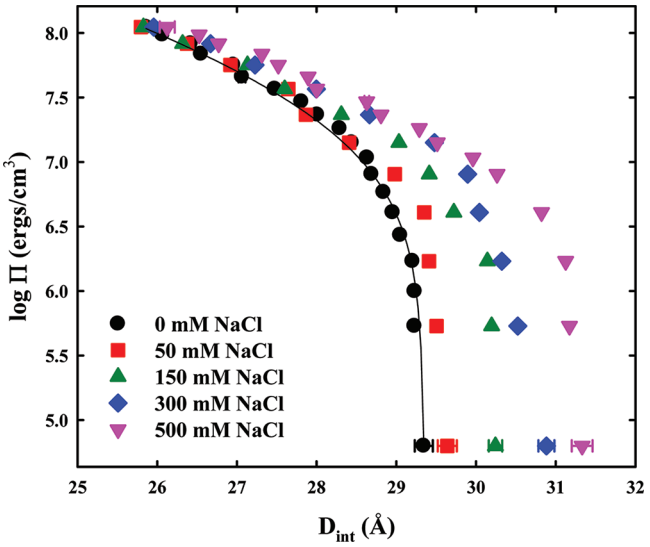


**Figure 3.** Osmotic stress force curves for protamine−DNA assemblies as dependent on NaCl concentration. Interhelical spacings are shown as a function of osmotic pressure of PEG applied on the DNA condensed phase for five NaCl concentrations. The solid line is a fit to the low salt data using a two-exponential formalism outlined previously[7−9] with fixed decay length $\lambda = 4.8$ Å. The force curves converge at high osmotic pressures. The points at $\log(\Pi) \sim 5$ represent spacings in the absence of PEG. Error bars are given for several points based on three measurements. The equilibrating solutions also contained 100 $\mu$M salmon protamine and 10 mM Tris (pH7.5) in addition to PEG and NaCl.

The change in the number of ions in the condensed DNA array as osmotic work is done can be estimated from the dependence of the spacing on PEG osmotic pressure and salt concentration through a Maxwell relation of the fundamental Gibbs−Duhem equation.

$$-d\mu_{DNA} = -V_w\, d\Pi + N_s\, d\mu_s \qquad (2)$$

where $\mu_{DNA}$ is the DNA chemical potential per bp, $\Pi$ is the osmotic pressure of PEG, $\mu_s$ is the salt chemical potential, and $V_w$ and $N_s$ are the volume of water and number of ions in the condensed DNA phase per bp. The Maxwell relation is then

$$\left.\frac{\partial N_s}{\partial \Pi}\right|_{\mu_s} = -\left.\frac{\partial V_w}{\partial \mu_s}\right|_{\Pi} \quad \text{or} \quad \Delta N_s = -\int_{\Pi_0}^{\Pi_1} \left.\frac{\partial V_w}{\partial \mu_s}\right|_{\Pi} d\Pi \qquad (3)$$

For hexagonal packing, the volume per bp is $V = (\sqrt{3}/2) D_{int}^2 l$, where $l$ is the distance between bp along the helix axis, assumed to be 3.4 Å. We assume that the change in volume from changing osmotic pressures and salt concentrations is dominated by water. Similarly, we approximate $d\mu_s$ as $kT\ d\ \ln(C_s)$, where $C_s$ is the molar concentration of salt.

We use NaBr to evaluate $\Delta N_s$ for protamine−DNA assemblies. Osmotic pressures of PEG and NaBr are additive, and NaBr activities are unchanged by PEG (both to within ~5%). Figure 4a shows the osmotic stress force curve for protamine−DNA without added NaBr and the effect of NaBr concentration on interhelical spacing at several PEG osmotic pressures. Once again, the spacings converge at higher pressures. Figure 4b shows the dependence of $V$ on $\ln(C_s)$ (eq 3) for the six pressures measured. Average slopes at 200 mM NaBr can be calculated. An upward curvature in these plots is particularly noticeable at low

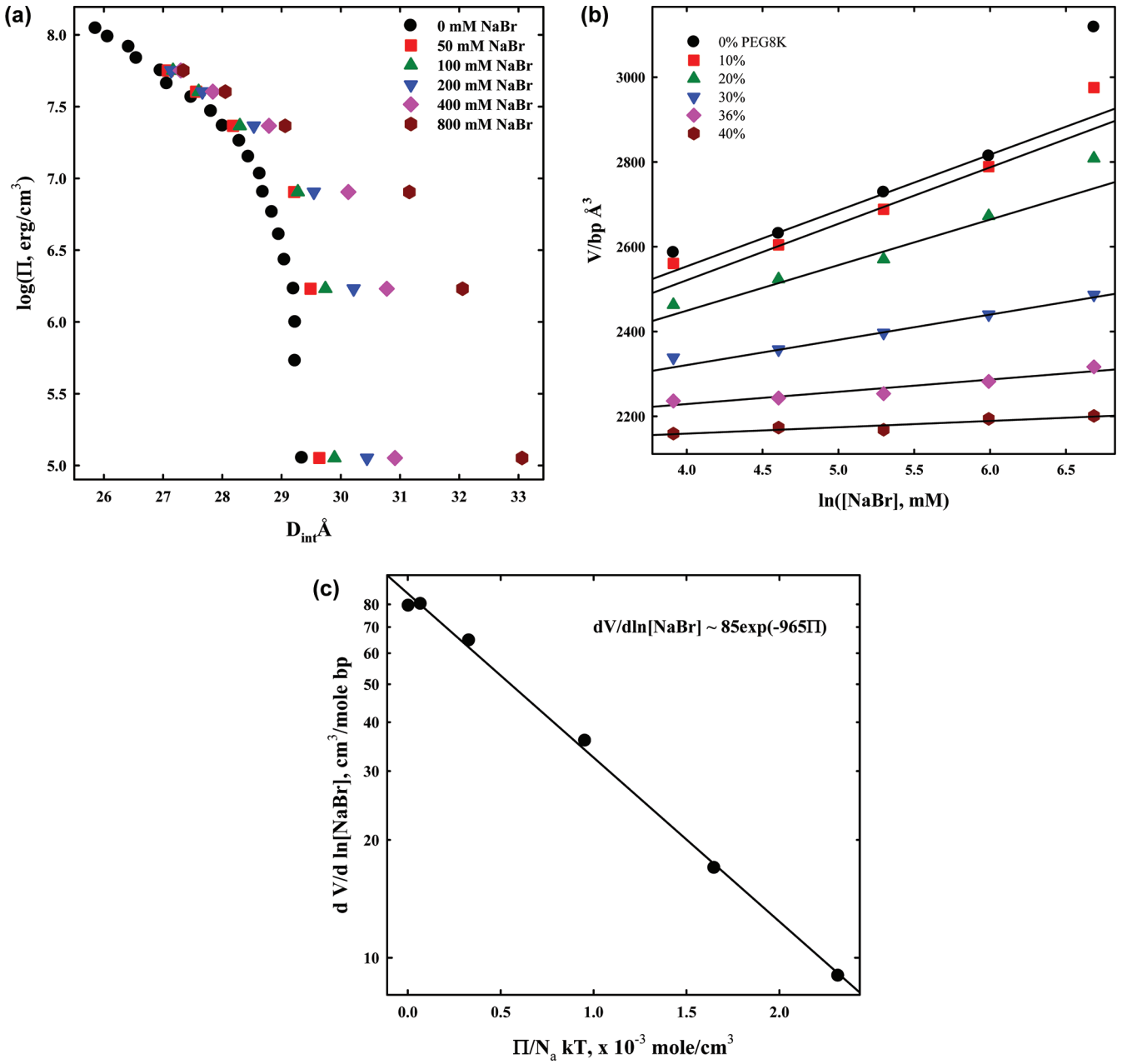


**Figure 4.** Quantitating the binding of $Br^-$ to condensed protamine−DNA arrays. (a) Osmotic pressure-vs-distance curves are shown for six pressures and six concentrations of NaBr. As in Figure 3, the data converges at high pressures. The points at $\log(\Pi) \sim 5$ actually represent the spacings in the absence of PEG. The equilibrating solutions also contained 100 $\mu$M salmon protamine and 10 mM Tris (pH 7.5) ,in addition to PEG and NaBr. (b) The volume associated with a base pair, $(\sqrt{3}/2)\, l\, \Delta(D_{int}^2)$ where $l$ = 3.4 Å, in the hexagonally packed array is plotted against ln([NaBr]) for the six PEG concentrations shown in panel a. Weight percentages of PEG are shown in the key. The lines show the best-fitting slopes at 200 mM NaBr. (c) The slopes determined in (b) are plotted against the modified osmotic pressure, $\Pi/N_A kT$, where $N_A$ is Avogadro's number. To a good approximation, the dependence is exponential. Integrating the curve from $\Pi = 0$ to $\infty$ gives the change in the number of $Br^-$ bound per DNA base pair.

osmotic pressures. This is indicative of an increasing number of "bound" $Br^-$'s with higher NaBr concentrations.

Figure 4c shows the dependence of $\ln(\partial V_w/\partial \ln(C_s))|_\Pi$ at 200 mM NaBr on $\Pi$. To a good first-order approximation, the dependence is single exponential. Integrating from $\Pi = 0$ to $\infty$ gives a net loss of 0.09 $Br^-$ ions per bp. Since one salmon protamine with 21 arginine charges neutralizes 10.5 bp, we estimate that initially 0.95 $Br^-$ ions were bound per protamine at 200 mM NaBr. This modest amount of binding (1 $Br^-$/21 arginine charges) was able to swell the DNA−protamine assembly by over 1 Å, or by more than 10% of the surface-to-surface distance.

The net energy associated with removing $Br^-$ due to compressing the DNA array from the equilibrium spacing $D_{eq}$ to some spacing $D_{int}$ can be calculated from the osmotic work, $\int_{D_{eq}}^{D_{int}} \sqrt{3l\Pi}\, dD$, difference between the $\Pi-V$ curves in 200 mM NaBr and with no added $Br^-$. Figure 5 shows the osmotic work difference as a function of the $\Delta N_{Br^-}$/protamine calculated from Figure 4b and eq 2. An exponential spline analysis was used to approximate the integrated work. This work is the balance between


dx.doi.org/10.1021/jp203834z |J. Phys. Chem. B 2011, 115, 11888–11894

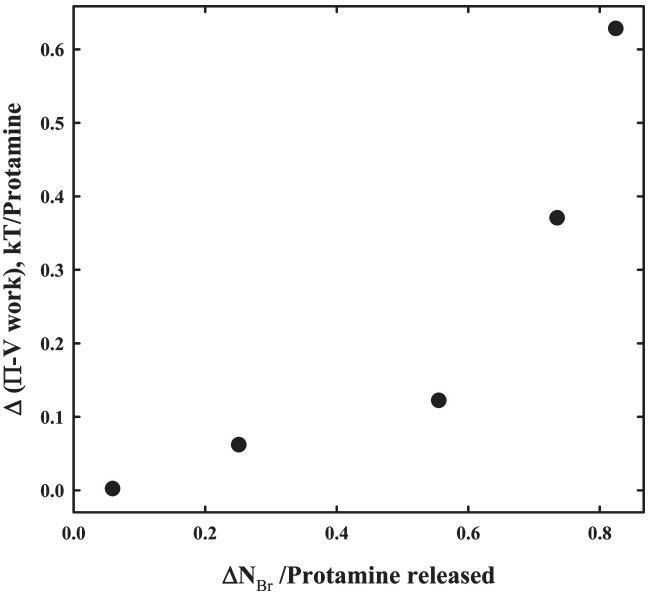


**Figure 5.** The Π−V work done in removing $Br^-$ from the protamine−DNA condensate. The difference $\Pi\Delta V$ work between the force curves with 200 mM NaBr and with no added NaBr is shown as a function of the number of $Br^-$'s removed per protamine. For each force curve, a work is calculated from Π = 0 to Π*, the PEG osmotic pressures actually used in the measurements. $\Delta N_{Br^-}$ is calculated by integrating the curve shown in Figure 4c from Π = 0 to Π*.

the energy gained in more favorable DNA−DNA interactions and the energy lost in releasing $Br^-$ as helices move closer. The work done increases dramatically as fewer and fewer $Br^-$ ions remain bound.

## DISCUSSION

Using a two-exponential formalism that fits a wide range of DNA−DNA force curves,[7−9] we have previously estimated the depth of the energy minimum for protamine−DNA arrays in minimal salt (10 mM Tris) as ∼0.7 kT/bp.[9] Since DNA is stiff, this modest attraction per base pair leads to strong assembly. The forces between protamine−DNA helices are, however, quite salt-concentration-dependent. The large difference in DNA−DNA spacings between NaSCN and NaOAc at 0.5 M and higher (Figure 2 and Table 1) indicates that the loss of attraction is due to specific anion binding. DNA−protamine arrays have increased nearly 19% by volume at 500 mM NaSCN while swelling less than 2% at the same concentration of NaOAc compared with 10 mM Tris salt. Within the two exponential formulism we developed,[7−9] the equilibrium spacing between helices and interhelical forces are determined by a balance between an ∼2.4 Å decay length repulsion and an ∼4.8 Å decay length attraction. Since we have not measured a force curve with a constant number of bound anions, we do not know if this loss of attraction is due to increased amplitude of the ∼2.4 Å decay length repulsion or to a decrease in the ∼4.8 Å decay length attraction.

It is now standard practice to characterize the precipitation of DNA by multivalent ions by measuring critical univalent salt/multivalent ion concentrations, that is, to determine a phase diagram. At the transition between soluble and condensed DNA, there is a free energy balance between the attractive energy gained in assembly and the unfavorable energy associated with the rearrangement of ions bound to soluble DNA. The attractive energy gained in the condensed phase due to binding of multiply charged ions increases the association binding constant of these ions compared with DNA in the bulk solution. The increase in multivalent ion binding upon condensation is accompanied by a consequent release of univalent salt. In interpreting the salt dependence of the critical multivalent ion concentration, it is implicitly assumed that the condensed phase is insensitive to salt concentration. As seen here, however, anion binding by protamine means that the multivalent ion species present in solution changes with salt concentration and that the nature and energetics of the condensed DNA are salt-dependent. Since attractive energy is lost as anions bind to protamine in the condensed DNA phase, anions will bind even more strongly to free protamine or protamine bound to soluble DNA than to protamine in the condensed DNA phase. This 2-fold action of salt, protamine binding, and competition with protamine for DNA binding greatly complicates any simple interpretation of the salt phase diagram.

With only one species of multivalent ion, $M^{n+}$, competing with only $Na^+$, then the interplay of $M^{n+}$ and $Na^+$ concentrations at the transition point is given by a relationship that can be derived from the Gibbs−Duhem equation for a phase transition,

$$\left.\frac{d\ln(C_{M^{n+}})}{d\ln(C_{Na^+})}\right|_{tr} \approx \left.\frac{d\mu_{M^{n+}}}{d\mu_{Na^+}}\right|_{tr} = -\frac{\Delta N_{Na^+}}{\Delta N_{M^{n+}}} \quad (4)$$

$\Delta N_{M^{n+}}$ and $\Delta N_{Na^+}$ are the differences in the numbers of $M^{n+}$ and $Na^+$ ions thermodynamically bound to DNA, respectively, between the soluble and condensed phases. The concentration $C_{M^{n+}}$ is the actual bulk solution concentration of $M^{n+}$. If all neutralizing ions were simply bound to DNA, then for each extra $M^{n+}$ ion that binds in the transition to the condensed phase, $n$ $Na^+$ ions are released, and the slope is $n$. It becomes more complicated if all ions are not directly bound to DNA. Neutralizing ions in the diffuse atmosphere, for example, count as only half-bound thermodynamically, as can be readily calculated from $d\,G_{el}/kT\,d\ln(C_{Na+})$, where $G_{el}$ is the DNA charging free energy in the Debye−Hückel limit for thin rods.

The process becomes much more complicated when the multivalent ion can bind anions to form $MX^{(n-1)+}$, $MX_2^{(n-2)+}$, etc. The transition to the condensed phase involves not only the displacement of $Na^+$ by the various multivalent ion species but also the displacement of lower-charged multivalent ion species with more highly charged species. Of course, the distribution of multivalent ion species depends on the overall salt concentration.

This balance of binding and release of ions at the transition point determines only the slope of $\ln(C_{M^{n+}})_{tr}$ vs $\ln(C_{Na^+})_{tr}$. Prediction of the absolute transition concentrations requires a more in-depth analysis of the balance of energies. The extent of the redistribution of ions between the soluble and condensed DNA phases depends on the change in DNA−DNA interaction energies, from repulsive in the soluble phase to attractive in condensed arrays. The swelling of the protamine−DNA condensed phase with increasing salt indicates a loss of attractive energy between helices as anions bind to protamines. Less extensive ion rearrangement can be supported by the decreased attractive energy.

These multivalent ions are, of course, highly charged in their own right. Salmon protamine has an overall nominal linear charge density of ∼1charge/ ∼4−6 Å, depending on extension, less charged than DNA, but still more than the Manning cutoff for condensation, ∼1 charge/7 Å. It is not surprising that protamines bind anions reasonably strongly. The binding of univalent anions is not, however, dominated by electrostatics, but

by a combination of electrostatics and anion chemistry. Of the univalent anions, the chaotropes $SCN^-$ and $I^-$ bind more strongly to protamine, presumably to the arginines with their terminal, chaotropic guanidinium groups. The kosmotropes $F^-$ and $OAc^-$ barely affect protamine−DNA forces until very high concentrations (>1.5 M). This is in qualitative agreement with solubilities of univalent inorganic salts.[27] Kosmotrope−kosmotrope and chaotrope−chaotrope pairs are less soluble than mixed kosmotrope−chaotrope pairs. For example, LiF (∼0.1 mol/kg water at ∼20 °C) is much less soluble than LiI (∼12.3 mol/kg water), but CsF (∼24.2 mol/kg water) is much more soluble than CsI (∼0.1 mol/kg water). The binding of divalent $SO_4^{2-}$ is quite strong, even though the anion is a strong kosmotrope. Presumably, the electrostatic contribution to divalent ion binding is stronger, although $SCN^-$ and $SO_4^{2-}$ binding effects differ by only a factor of 2 in anion concentration. Although not studied extensively, qualitatively similar behavior was observed for the effect of different salts on polylysine−DNA and polyarginine−DNA forces; $F^-$ and $OAc^-$ affect $D_{int}$ less than $SCN^-$ and $SO_4^{2-}$.

The extent of swelling before dissolution also seems dependent on the salt species (Figure 2). The spacing at which pellets will dissolve depends on the net attractive energy. $Arg_2$−DNA arrays undergo a transition from repulsion to attraction at low osmotic pressures.[9] These data can be used to estimate the minimal free energy necessary to maintain a condensed phase. We estimated from curve-fitting an equilibrium spacing and net free energy at $\Pi = 0$ after the transition of 34.2 Å and −0.05 kT/bp. The net free energy, in turn, depends sensitively on the magnitudes of the component ∼2.4 and ∼4.8 Å exponential decay length forces. The increase in spacing with salt concentration seen in Figure 2 can have two causes: the binding of anions to protamine and the displacement of protamine from the DNA phase by salt. The effect of $SCN^-$ and $SO_4^{2-}$ is presumably dominated by anion binding, although NaOAc at ∼2 M likely acts through protamine displacement by $Na^+$ competition. The very different spacings at the critical point for pellet dissolution would indicate that anion binding and $Na^+$ competition have different effects on the ∼2.4 and ∼4.8 Å decay length force coefficients. The salt dependence of the interaxial spacing and the salt concentration at which pellets dissolve at $\Pi = 0$, however, can be calculated only if the changes in the amplitudes of the ∼2.4 and ∼4.8 Å decay length forces accompanying the constant anion binding or $Na^+$ displacement are known. The interplay of osmotic pressure and protamine anion binding or $Na^+$−protamine competition, however, makes this impractical.

The osmotic stress force curves are sensitive to anion concentration. The difference in $\Pi\Delta V$ work done in moving helices closer with and without added salt changes the anion binding free energy. The loss of bound anions as helices are pushed closer can be calculated through a Maxwell relation linking the change in volume between helices as the PEG osmotic pressure is varied to the number of anions bound and the chemical potential of the salt. We quantitated the loss of $Br^-$ binding at ∼200 mM NaBr in this way. At this concentration, ∼1 $Br^-$ is bound per protamine at $\Pi = 0$. Judging from the curvature of the $V$ vs $\ln(C_{NaBr})$ plot in Figure 4b, even more bind at higher concentrations.

The effect of anion binding on forces is remarkable. This 1 bound $Br^-$ per 21 arginine charges shifts the spacing between helices by ∼1.1 Å, or almost 12% of the surface-to-surface distance between helices. We estimate from Figure 4 that the net $\Pi\Delta V$ work done in releasing 90−95% of this bound $Br^-$ at very high pressures and close DNA spacings is ∼1 kT. This net energy can be separated into DNA−DNA interaction and $Br^-$ binding energies only with an additional $\Pi$-D force curve with one $Br^-$ bound per protamine present at all pressures.

## CONCLUSIONS

In this work, we have explored the effect of salt on condensed DNA assemblies. Using osmotic stress, we have directly probed the salt sensitivity of the intermolecular forces between helices in condensed protamine−DNA arrays. Both anion binding and cation screening or competition weaken the attractive forces between DNA helices mediated by bound protamine. The strength of anion binding follows the Hofmeister series, with chaotropic anions binding more tightly to protamine−DNA arrays than kosmotropic anions. Although specific cation effects are observed, they are small compared with anion effects. Through a Gibbs−Duhem relationship, we were able to directly estimate the number of ions bound in the condensed phase without applied osmotic pressure. For 200 mM NaBr salt concentration at equilibrium, we estimate one $Br^-$ anion is bound per protamine chain. This one bound anion weakens DNA−DNA attractions sufficiently to induce a surprisingly large ∼12% increase in the surface-to-surface distance between DNA helices.

This sensitivity of attraction to bound anions has possible biological significance. Protamine serines are phosphorylated before binding to DNA in spermatogenesis.[2,6] Sulfate binding that very strongly weakens DNA−DNA attraction might closely mimic the effect of protamine phosphorylation. The DNA−DNA forces with bound phosphorylated protamines would then be expected to have a significantly weaker attraction than unmodified protamine and be less able to compete with NaCl or perhaps will even be repulsive, depending on the extent of phosphorylation. Orderly dephosphorylation of phosphorylated protamine offers the possibility of an orderly folding of protamine−DNA into the structures found in sperm nuclei.

## MATERIALS AND METHODS

**Reagents.** Polyethylene glycol, average molecular weights (MW) of 8000 was purchased from Fluka Chemical (Buchs, Switzerland). Salmon protamine chloride was purchased from the Sigma Chemical Company and used without further purification. All salts used were analytic grade. High molecular weight DNA ($MW > 5 \times 10^6$) was prepared and purified from adult chicken whole blood as described previously[7] and stored in 10−1 TE (10 mM TrisCl (pH 7.5), 1 mM EDTA). We are not aware of any evidence indicating that DNA−DNA forces are dependent on DNA molecular weight. DNA−DNA forces measured in $Na^+$, spermidine, and spermine are the same for high molecular weight DNA and for nucleosomal 150 bp DNA (unpublished observations). The equilibrium interhelical spacing for spermine assembled DNA is the same for high molecular weight DNA,[18] for 150 bp DNA,[17] and for 25 bp oligonucleotides;[28] all are in very good agreement.

**Sample Preparation.** Protamine−DNA spontaneously precipitates, and samples for X-ray scattering were prepared in two ways. Protamine solution (∼2 mM) was added to 200 μL of ∼1 mg/mL chicken erythrocyte DNA (∼250 μg DNA) in 10 mM TrisCl (pH 7.5) in steps of ∼0.2 protamine charge/DNA charge. Each addition was thoroughly mixed before adding more condensing ions and continued until all DNA was precipitated. Alternatively, protamine was added to DNA in a single aliquot to an equivalent final concentration. The resulting fibrous samples

were centrifuged and transferred to corresponding PEG−salt solutions with 100 $\mu$M excess protamine and 10 mM Tris (ph 7.5) and allowed to equilibrate for approximately 2 weeks. X-ray scattering profiles did not depend on the method used to prepare the DNA precipitate and did not change after 6 months. Osmotic pressures of the PEG−salt solutions were measured directly using a Vapro vapor pressure osmometer (model 5520, Wescor, Logan, UT). For the osmotic stress measurements, control experiments were performed to ensure that osmotic pressure is the pertinent variable.[20,29]

**X-ray Scattering.** Both an Oxford Instruments microfocus UltraBright X-ray source and an Enraf-Nonius Service Corp. (Bohemia, NY) fixed copper anode Diffractis 601 X-ray generator equipped with double focusing mirrors (Charles Supper Co.) were used for X-ray scattering. DNA samples were sealed with a small amount of equilibrating solution in the sample cell and then mounted into a temperature-controlled holder at 20 °C, as described in Mudd et al.[30] The sample-to-film distance was ∼16 cm. The scattered X-rays pass through a helium-filled Plexiglas cylinder with Mylar windows to minimize background scattering. Diffraction patterns were recorded by direct exposure of Fujifilm BAS image plates and digitized with a Fujifilm FLA 3000 scanner. The images were analyzed using the FIT2D (copyright A. P. Hammersley, ESRF) and SigmaPlot 10.0 (SPSS Inc.). The sample-to-image plate distance was calibrated using powdered *p*-bromobenzoic acid. Mean pixel intensities between scattering radii $r-.05$ mm and $r+.05$ mm averaged over all angles of the powder pattern diffraction, $\langle I(r)\rangle$, were used to calculate integrated radial intensity profiles, $2\pi r\langle I(r)\rangle$.

## AUTHOR INFORMATION

### Corresponding Author

*E-mail: raud@mail.nih.gov or derouchey@uky.edu.

## ACKNOWLEDGMENT

This research was supported by the Intramural Research Program of the Eunice Kennedy Shriver National Institute of Child Health and Human Development, National Institutes of Health.

## REFERENCES

(1) Pogany, G. C.; Corzett, M.; Weston, S.; Balhorn, R. *Exp. Cell Res.* **1981**, *136*, 127–136.
(2) Balhorn, R. *Genome Biology* **2007**, *8*.
(3) Wyrobek, A. J.; Meistrich, M. L.; Furrer, R.; Bruce, W. R. *Biophys. J.* **1976**, *16*, 811–825.
(4) Robinson, P. J. J.; Fairall, L.; Huynh, V. A. T.; Rhodes, D. *Proc. Natl. Acad. Sci. U.S.A.* **2006**, *103*, 6506–6511.
(5) Blanc, N. S.; Senn, A.; Leforestier, A.; Livolant, F.; Dubochet, J. *J. Struct. Biol.* **2001**, *134*, 76–81.
(6) Lewis, J. D.; Song, Y.; de Jong, M. E.; Bagha, S. M.; Ausio, J. *Chromosoma* **2003**, *111*, 473–482.
(7) Rau, D. C.; Parsegian, V. A. *Biophys. J.* **1992**, *61*, 246–259.
(8) Todd, B. A.; Parsegian, V. A.; Shirahata, A.; Thomas, T. J.; Rau, D. C. *Biophys. J.* **2008**, *94*, 4775–4782.
(9) DeRouchey, J.; Parsegian, V. A.; Rau, D. C. *Biophys. J.* **2010**, *99*, 2608–2615.
(10) Raspaud, E.; de la Cruz, M. O.; Sikorav, J. L.; Livolant, F. *Biophys. J.* **1998**, *74*, 381–393.
(11) Pelta, J.; Livolant, F.; Sikorav, J. L. *J. Biol. Chem.* **1996**, *271*, 5656–5662.
(12) Korolev, N.; Berezhnoy, N. V.; Eom, K. D.; Tam, J. P.; Nordenskiold, L. *Nucleic Acids Res.* **2009**, *37*, 7137–7150.
(13) Toma, A. C.; de Frutos, M.; Livolant, F.; Raspaud, E. *Biomacromolecules* **2009**, *10*, 2129–2134.
(14) Makita, N.; Yoshikawa, Y.; Takenaka, Y.; Sakaue, T.; Suzuki, M.; Watanabe, C.; Kanai, T.; Kanbe, T.; Imanaka, T.; Yoshikawa, K. *J. Phys. Chem. B* **2011**, *115*, 4453–4459.
(15) Todd, B. A.; Rau, D. C. *Nucleic Acids Res.* **2008**, *36*, 501–510.
(16) Wilson, R. W.; Bloomfield, V. A. *Biochemistry* **1979**, *18*, 2192–2196.
(17) Raspaud, E.; Durand, D.; Livolant, F. *Biophys. J.* **2005**, *88*, 392–403.
(18) Yang, J.; Rau, D. C. *Biophys. J.* **2005**, *89*, 1932–1940.
(19) Saito, T.; Iwaki, T.; Yoshikawa, K. *Biophys. J.* **2009**, *96*, 1068–1075.
(20) Parsegian, V. A.; Rand, R. P.; Fuller, N. L.; Rau, D. C. *Methods Enzymol.* **1986**, *127*, 400–416.
(21) Marushige, Y.; Marushige, K. *Biochim. Biophys. Acta* **1978**, *518*, 440–449.
(22) Pruslin, F. H.; Imesch, E.; Winston, R.; Rodman, T. C. *Gamete Res.* **1987**, *18*, 179–190.
(23) Green, G. R.; Balhorn, R.; Poccia, D. L.; Hecht, N. B. *Mol. Reprod. Dev.* **1994**, *37*, 255–263.
(24) Fita, I.; Campos, J. L.; Puigjaner, L. C.; Subirana, J. A. *J. Mol. Biol.* **1983**, *167*, 157–177.
(25) Podgornik, R.; Strey, H. H.; Gawrisch, K.; Rau, D. C.; Rupprecht, A.; Parsegian, V. A. *Proc. Natl. Acad. Sci. U.S.A.* **1996**, *93*, 4261–4266.
(26) DeRouchey, J.; Netz, R. R.; Radler, J. O. *Eur. Phys. J. E* **2005**, *16*, 17–28.
(27) Collins, K. D.; Washabaugh, M. W. *Q. Rev. Biophys.* **1985**, *18*, 323–422.
(28) Qiu, X.; Andresen, K.; Lamb, J. S.; Kwok, L. W.; Pollack, L. *Phys. Rev. Lett.* **2008**, *101*, 228101.
(29) Rau, D. C.; Lee, B.; Parsegian, V. A. *Proc. Natl. Acad. Sci. U.S.A.* **1984**, *81*, 2621–2625.
(30) Mudd, C. P.; Tipton, H.; Parsegian, A. V.; Rau, D. *Rev. Sci. Instrum.* **1987**, *58*, 2110–2114.